

# Retroreflector with acute dihedral angles

Nobuo Sugimoto and Atsushi Minato

National Institute for Environmental Studies, 16-2 Onogawa, Tsukuba, Ibaraki 305, Japan

Received May 9, 1994

An acute-angle retroreflector having three dihedral angles of 45, 60, and 90 deg was studied by use of the ray-trace method. Incident rays are reflected nine times in the retroreflector, and there are 26 different sequences for reflections. Errors in the dihedral angles will cause the directions of the reflected rays to diverge. A possible application of the acute-angle retroreflector is in target design for laser ranging.

A hollow cube-corner retroreflector is formed with three mirrors connected to one another at right angles. It reflects incident rays exactly in the opposite direction. Incident rays are effectively reflected at the apex of the corner cube, which we call the origin of reflection in the following discussion. Three mirrors connected with two right dihedral angles and one acute dihedral angle, 45 deg, for example, form a retroreflector. The value of the acute angle at which the optical system works as a retroreflector is  $90/N$  deg, where  $N$  is an integer. When this condition is met, a virtual corner cube is formed by the reflections of the mirrors.

With similar symmetrical considerations, we searched for retroreflectors having two or more acute dihedral angles. We found that the only combination of three dihedral angles that forms a retroreflector is that of 90, 60, and 45 deg. For an optical system consisting of three mirrors to work as a retroreflector, two conditions must be satisfied. First, the virtual space inside the optical system must be filled consistently with mirror images of the optical system itself. Second, the virtual element on the opposite side must have point symmetry with the real optical system. One can find such shapes by cutting a corner cube with symmetrical planes. Figure 1 shows the shapes that satisfy the conditions and how the conditions are satisfied. All elements in Fig. 1 have mirror symmetry with respect to the intervening surfaces. There are two symmetrical types of acute-angle retroreflectors, as illustrated in Fig. 2. They are triangular pyramids that are one-sixth portions of a corner cube.

We studied the acute-angle retroreflector by the ray-trace method. We chose the type shown in Fig. 2(a) for our study because both types have essentially the same optical characteristics. We denoted mirrors 1, 2, and 3; three dihedral angles  $\theta_1$ ,  $\theta_2$ , and  $\theta_3$ ; and vectors  $x_1$ ,  $x_2$ , and  $x_3$ , as indicated in Fig. 2(a). The angles between vectors  $x_1$  and  $x_2$ ,  $x_2$  and  $x_3$ , and  $x_3$  and  $x_1$  are 54.74, 35.26, and 45 deg, respectively.

The usual cube-corner retroreflector has six different sequences for reflections with three mirrors.<sup>1</sup> We found in the ray-trace study that an incident ray is reflected nine times in the acute-angle retroreflector and that there are 26 different sequences for reflections, depending on the position of the incident ray. Consequently, the aperture of the reflector can

be divided into 26 domains based on the order of reflections.

The number of reflections and the number of domains can be understood from Fig. 1. We can consider a ray that penetrates the virtual retroreflectors of Fig. 1 instead of tracing a ray that changes direction at each reflection in the real retroreflector. The mirror surfaces of the virtual retroreflectors in Fig. 1 are formed with nine planes that pass through the origin, and there are 26 intersections between the

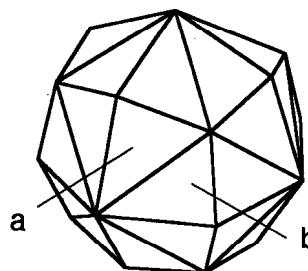


Fig. 1. Shapes that work as retroreflectors and their mirror images. Two types of the acute-angle retroreflector are indicated by the letters a and b.

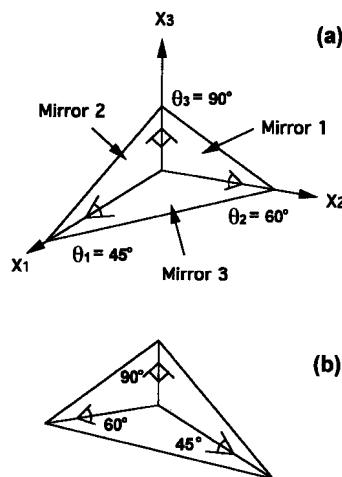


Fig. 2. Acute-angle retroreflectors. There are two symmetrical types.

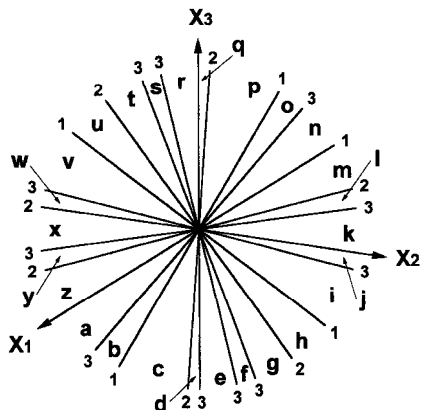


Fig. 3. Acute-angle retroreflector viewed from the direction of  $(x_1 + x_2 + x_3)/\sqrt{3}$ . The aperture can be divided into 26 domains based on the sequence for reflections.

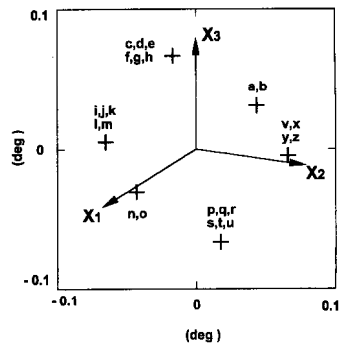
Table 1. Order of Reflections in the Acute-Angle Retroreflector

Domain	1	2	3	4	5	6	7	8	9
a	3	2	3	2	1	3	2	3	1
b	3	2	3	1	2	3	2	3	1
c	3	2	3	1	3	2	3	2	1
d	3	2	1	3	1	2	3	2	1
e	3	2	1	3	1	2	3	1	2
f	3	2	1	3	2	1	3	1	2
g	3	1	2	3	2	1	3	1	2
h	3	1	2	3	2	3	1	3	2
i	3	1	3	2	3	2	1	3	2
j	3	1	3	2	3	1	2	3	2
k	1	3	1	2	3	1	2	3	2
l	1	3	2	1	3	1	2	3	2
m	1	3	2	3	1	3	2	3	2
n	1	3	2	3	1	2	3	2	3
o	1	3	2	3	2	1	3	2	3
p	1	2	3	2	3	1	3	2	3
q	1	2	3	2	1	3	1	2	3
r	2	1	3	2	1	3	1	2	3
s	2	1	3	1	2	3	1	2	3
t	2	1	3	1	2	3	2	1	3
u	2	3	1	3	2	3	2	1	3
v	2	3	1	2	3	2	3	1	3
w	2	3	2	1	3	2	3	1	3
x	2	3	2	1	3	2	1	3	1
y	2	3	2	1	3	1	2	3	1
z	2	3	2	3	1	3	2	3	1
a	3	2	3	2	1	3	2	3	1

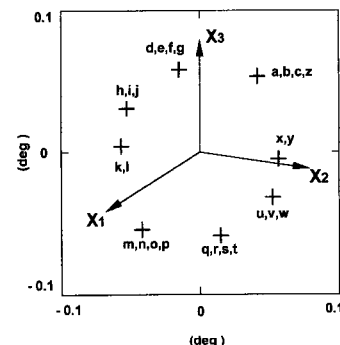
planes. Those numbers correspond to the number of reflections and the number of domains.

Figure 3 shows the central portion of the retroreflector viewed from the front of the reflector, which we define as the direction of the average of the vectors  $x_1$ ,  $x_2$ , and  $x_3$ , or  $(x_1 + x_2 + x_3)/\sqrt{3}$ . The lines shown in Fig. 3 indicate the three dihedral corners between mirrors and their mirror images. The numbers 1, 2, and 3 on the lines show that the lines are the mirror images of  $x_1$ ,  $x_2$ , and  $x_3$ , respectively. The domains are indicated by the letters a–z.

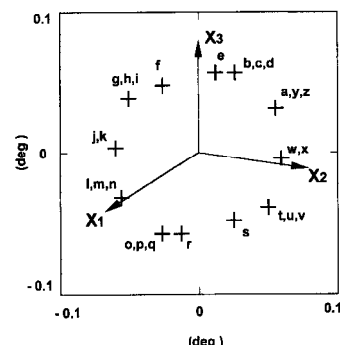
The order of reflections for a ray incident upon each domain is listed in Table 1. The numbers in Table 1 indicate the mirrors that are defined in Fig. 2(a). A ray is always reflected three times at mirror 2, but it



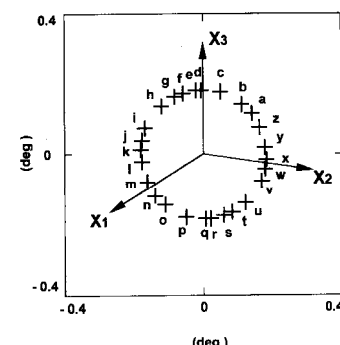
(a)



(b)



(c)



(d)

Fig. 4. Direction of the reflected rays when dihedral angle errors are introduced. An error of +0.01 deg is added to (a)  $\theta_1$ , (b)  $\theta_2$ , (c)  $\theta_3$ , (d)  $\theta_1$ ,  $\theta_2$ , and  $\theta_3$ .

is reflected two or three times at mirror 1 and three or four times at mirror 3, depending on the sequence.

We studied the effect of errors in dihedral angles. The reflected ray is exactly in the opposite direction to the incident ray when there is no error in the dihedral angles. If errors are introduced, the direction of the reflected ray changes, depending on the reflection sequence. Figures 4(a)–4(d) show the direction of the reflected ray for a ray incident upon each domain. The direction of incidence is  $(x_1 + x_2 + x_3)/\sqrt{3}$ . In Figs. 4(a)–4(c) an error of +0.01 deg is added to dihedral angles  $\theta_1$ ,  $\theta_2$ , and  $\theta_3$ ; in Fig. 4(d) an error of +0.01 deg is added to each dihedral angle. When an error is introduced in  $\theta_1$ , the reflected rays split into 6 directions. The rays split into 8 directions when an error is introduced in  $\theta_2$  and into 12 directions when an error is introduced in  $\theta_3$ . When errors are introduced in all the dihedral angles, the rays split into 26 directions.

The splitting of the reflected rays can be explained by reference to Table 1. The reflection sequences 1, 2, and 2, 1 represent the retroreflections at the corner with a 90-deg dihedral angle. These retroreflections are equivalent in regard to the direction of the reflected ray if there is no error in the dihedral angle. In the same manner, the reflection sequences 3, 1, 3 and 1, 3, 1 represent the retroreflections at the corner with a 60-deg dihedral angle, and they are equivalent if there is no angle error. Also, the sequences 2, 3, 2, 3 and 3, 2, 3, 2 represent the retroreflections at the corner with a 45-deg dihedral angle, and they are equivalent if there is no angle error. These sequences are marked in Table 1. If an error is introduced in  $\theta_1$ , the sequences 1, 2 and 2, 1 are no longer equivalent. As a result, the output rays will split. Consequently, we can see, for example, that the directions of the reflected rays for sequences a and b in Table 1 will be different. Also, there will be differences between d and e, e and f, f and g, i and j, k and l, etc. The splitting can be explained for errors in  $\theta_2$  and  $\theta_3$  in the same way.

The splitting can also be explained by referring to Fig. 3. The reflection of rays incident upon the domains on both sides of  $x_1$  or the mirror images of  $x_1$  are not equivalent when an error is introduced in  $\theta_1$ . It can be explained in the same way for  $\theta_2$  and  $\theta_3$ .

A possible application of the acute-angle retroreflectors is in a single-origin retroreflector array in which all elements of the array have an identical origin. The single-origin retroreflector array is useful as a laser ranging target, which is used from multiple directions at the same time. It may also be useful as a target for satellite laser ranging because it can be designed so that the origin of the reflection coincides with the center of gravity of the satellite. A single-origin retroreflector array can also be formed with general corner cubes, but the number of elements is limited. The number is limited to three when the elements are placed circularly because of the thickness of the mirrors. It is limited to four when the elements are placed on a sphere with the symmetry of a regular polyhedron. The number of elements can be increased by use of the acute-angle retroreflector. An array that has 20 elements on a sphere can be designed with acute-angle retroreflectors.

One of the features of the acute-angle retroreflector is that the reflected beam splits almost conically when errors are introduced, as shown in Fig. 4(d). This effect can be utilized for optimizing the reflected beam in the design of a satellite laser ranging target. We are investigating the far-field pattern of the acute-angle retroreflector with a wave-front calculation. We are also studying the effect of using curved mirrors<sup>2</sup> in the acute-angle retroreflector.

## References

1. D. A. Thomas and J. C. Wyant, *J. Opt. Soc. Am.* **67**, 467 (1977).
2. A. Minato, N. Sugimoto, and Y. Sasano, *Appl. Opt.* **31**, 6015 (1992).